Design and analysis of In$_{0.53}$Ga$_{0.47}$As/InP symmetric gain optoelectronic mixers

Wang Zhang [a], Nuri W. Emanetoglu [a,*], Neal Bambha [b], Justin R. Bickford [b]

[a] Electrical and Computer Engineering, University of Maine, USA
[b] Sensors and Electron Devices Directorate, Army Research Laboratory, USA

ABSTRACT

A symmetric gain optoelectronic mixer based on an indium gallium arsenide (In$_{0.53}$Ga$_{0.47}$As)/indium phosphide (InP) symmetric heterojunction phototransistor structure is being investigated for chirped-AM laser detection and ranging (LADAR) systems operating in the "eye-safe" 1.55 µm wavelength range. Signal processing of a chirped-AM LADAR system is simplified if the photodetector in the receiver is used as an optoelectronic mixer (OEM). Adding gain to the OEM allows the following transimpedance amplifier's gain to be reduced, increasing bandwidth and improving the system's noise performance. A symmetric gain optoelectronic mixer based on a symmetric phototransistor structure using an indium gallium arsenide narrow bandgap base and indium phosphide emitter/collector layers is proposed. The devices are simulated with the Synopsis TCAD Sentaurus tools. The effects of base–emitter interface layers, base thickness and the doping densities of the base and emitters on the device performance are investigated. AC and DC simulation results are compared with a device model. Improved responsivity and lower dark current are predicted for the optimized InGaAs/InP device over previously reported devices with indium aluminum arsenide emitter/collector layers.

1. Introduction

Optoelectronic mixing devices mix a modulated optical signal with a reference electrical signal to obtain an electrical low frequency difference signal. These devices are particularly attractive for chirped-AM laser detection and ranging (LADAR) systems. The Army Research Laboratory (ARL) has been developing chirped-AM LADAR systems for applications such as reconnaissance, terrain mapping, force protection, facial recognition, robotic navigation and weapons fuzing [1]. In this system, the amplitude of the laser beam is modulated with a chirped frequency local oscillator (LO) signal. The reflected laser beam is detected by a photodetector, which converts it into an electrical signal (RF). This time delayed RF will be at a different frequency than the instantaneous LO, with the difference frequency (f_{IF}) determined by the distance to target, the frequency bandwidth, ΔF, of the chirp, and its duration, T. Therefore, the RF signal is mixed with the IF signal to obtain the difference signal, and thus distance information. Signal processing of a chirped-AM LADAR system is simplified if the photodetector in the receiver is used as an optoelectronic mixer (OEM) [2]. A DC biased phototransistor can be used as an optoelectronic mixer [3]. Alternatively, a photodetector with a symmetric I–V characteristic allows driving the OEM directly with the local oscillator signal, without a DC bias [2]. Sensitivity to background light is reduced, as

the response from background light averages to zero. An additional 3 dB signal processing gain is also obtained. As the OEM output is the low frequency difference signal, the gain of the following transimpedance amplifier (TZA) can be increased, improving LADAR performance. ARL has previously demonstrated chirped-AM LADAR systems with GaAs and InGaAs metal–semiconductor–metal (MSM) Schottky photodetector OEMs for operation at the 800 nm [2,4] and 1550 nm wavelengths [5,6]. A symmetric photodetector with gain would improve overall system performance, while preserving the advantages offered by MSM OEM devices.

We previously reported Symmetric Gain OptoElectronic Mixers (SG-OEMs) for 1.55 µm operation based on a symmetric heterojunction phototransistor using In$_{0.52}$Al$_{0.48}$As/In$_{0.53}$Ga$_{0.47}$As heterostructures [7]. The emitter/collector was In$_{0.52}$Al$_{0.48}$As (InAlAs), and the base was In$_{0.53}$Ga$_{0.47}$As (InGaAs), both of which are lattice matched to the InP substrate. Two-dimensional device simulations, using the Synopsis TCAD Sentaurus suite, were carried out at the University of Maine to design optoelectronic mixers with suitable optical gain and frequency bandwidth. Two symmetric gain OEM heterostructures were grown at ARL using molecular beam epitaxy, and prototype devices were fabricated. Device diameters ranged from 18 µm to 30 µm. Etch steps during device fabrication revealed cracking defects in the thin films. Therefore, an investigation into an alternative device structure with InP layers was initiated to improve lattice-matching with the substrate and to reduce the defect density in the thin films.

* Corresponding author. Tel.: +1 207 581 2233.
E-mail address: nuri.emanetoglu@maine.edu (N.W. Emanetoglu).

Report Documentation Page	*Form Approved* *OMB No. 0704-0188*

Public reporting burden for the collection of information is estimated to average 1 hour per response, including the time for reviewing instructions, searching existing data sources, gathering and maintaining the data needed, and completing and reviewing the collection of information. Send comments regarding this burden estimate or any other aspect of this collection of information, including suggestions for reducing this burden, to Washington Headquarters Services, Directorate for Information Operations and Reports, 1215 Jefferson Davis Highway, Suite 1204, Arlington VA 22202-4302. Respondents should be aware that notwithstanding any other provision of law, no person shall be subject to a penalty for failing to comply with a collection of information if it does not display a currently valid OMB control number.

1. REPORT DATE **09 JUN 2010**	2. REPORT TYPE	3. DATES COVERED **00-00-2010 to 00-00-2010**
4. TITLE AND SUBTITLE **Design and analysis of In0.53Ga0.47As/InP symmetric gain optoelectronic mixers**		5a. CONTRACT NUMBER
		5b. GRANT NUMBER
		5c. PROGRAM ELEMENT NUMBER
6. AUTHOR(S)		5d. PROJECT NUMBER
		5e. TASK NUMBER
		5f. WORK UNIT NUMBER
7. PERFORMING ORGANIZATION NAME(S) AND ADDRESS(ES) **Army Research Laboratory,Sensors and Electron Devices Directorate,Adelphi,MD,20783**		8. PERFORMING ORGANIZATION REPORT NUMBER
9. SPONSORING/MONITORING AGENCY NAME(S) AND ADDRESS(ES)		10. SPONSOR/MONITOR'S ACRONYM(S)
		11. SPONSOR/MONITOR'S REPORT NUMBER(S)

12. DISTRIBUTION/AVAILABILITY STATEMENT **Approved for public release; distribution unlimited**

13. SUPPLEMENTARY NOTES

14. ABSTRACT

A symmetric gain optoelectronic mixer based on an indium gallium arsenide (In0.53Ga0.47As)/indium phosphide (InP) symmetric heterojunction phototransistor structure is being investigated for chirped- AM laser detection and ranging (LADAR) systems operating in the ??eye-safe? 1.55 lm wavelength range. Signal processing of a chirped-AM LADAR system is simplified if the photodetector in the receiver is used as an optoelectronic mixer (OEM). Adding gain to the OEM allows the following transimpedance amplifier?s gain to be reduced, increasing bandwidth and improving the system?s noise performance. A symmetric gain optoelectronic mixer based on a symmetric phototransistor structure using an indium gallium arsenide narrow bandgap base and indium phosphide emitter/collector layers is proposed. The devices are simulated with the Synopsis TCAD Sentaurus tools. The effects of base?emitter interface layers base thickness and the doping densities of the base and emitters on the device performance are investigated. AC and DC simulation results are compared with a device model. Improved responsivity and lower dark current are predicted for the optimized InGaAs/InP device over previously reported devices with indium aluminum arsenide emitter/collector layers.

15. SUBJECT TERMS					
16. SECURITY CLASSIFICATION OF:			17. LIMITATION OF ABSTRACT	18. NUMBER OF PAGES	19a. NAME OF RESPONSIBLE PERSON
a. REPORT **unclassified**	b. ABSTRACT **unclassified**	c. THIS PAGE **unclassified**	**Same as Report (SAR)**	**5**	

Standard Form 298 (Rev. 8-98)
Prescribed by ANSI Std Z39-18

In this work, InP/In$_{0.53}$Ga$_{0.47}$As heterostructure based symmetric gain optoelectronic mixers are investigated through simulation using the Synopsis TCAD Sentaurus tools. A symmetric gain optoelectronic mixer for the chirped-AM LADAR applications should have high responsivity below 5 V (peak voltage for 24 dBm LO signal) and low dark current. In comparison with In$_{0.52}$Al$_{0.48}$As, InP has a smaller bandgap difference with In$_{0.53}$Ga$_{0.47}$As and a different conduction band offset. Thus, comparative simulations are carried out to investigate the advantages and disadvantages of InP based SG-OEMs in comparison with InAlAs based ones. The two-dimensional simulations are used to design both the layer structure for growth and the horizontal structure for the photolithography masks. The simulations predict a higher responsivity for the InP based SG-OEMs, as well as a smaller dark current, hence lower noise floor. Highly doped base–emitter interface layers are investigated for improving device performance, as previously predicted for InAlAs based SG-OEMs. The base width and base–emitter doping dependence of the dark current and responsivity are also investigated to optimize the device structure for high responsivity, low leakage current, and a large breakdown voltage.

2. Simulation and modeling

2.1. DC simulation and analysis

The two basic device structures, with and without the emitter-side highly doped interface layer, are shown in Fig. 1, for the case of InP emitter/collector layers. Structure A has 10 nm thick highly doped InP interface layers between the base and emitter/collector layers, while structure B does not. The base layer thickness and the doping levels of the base and emitter layers are the main parameters varied in the device simulations. The material parameters used in the simulation are listed in Table 1.

Table 1
List of material parameters used in the simulations.

	InGaAs	InP	InAlAs
E_g (eV)	0.718721	1.33587	1.48159
χ_0 (eV)	4.5472	4.4	4.2711
ε_r	13.9061	12.4	12.3948
N_c (cm^{-3})	2.5396×10^{17}	5.66×10^{17}	5.7814×10^{17}
N_v (cm^{-3})	7.5107×10^{18}	2.03×10^{19}	9.4152×10^{18}

A large and symmetric gain, low leakage current, and a breakdown voltage larger than 5 V are the important specifications for an optoelectronic mixer in LADAR applications. An OEM with large gain would allow the following transimpedance amplifier's gain to be reduced, increasing the TZA frequency bandwidth and improving overall system performance. Fig. 2 compares the simulated responsivity versus bias voltage of InP and In$_{0.52}$Al$_{0.48}$As based SG-OEMs with the same layer thickness and doping profile, while their dark current performance is compared in Fig. 3. The simulations predict that InP based SG-OEMs will have a lower dark current, and be less susceptible to the Early effect and punch-through breakdown. The InP/In$_{0.53}$Ga$_{0.47}$As based structure A device has a base width of 800 nm, base doping of 2.5×10^{16} cm^{-3} and collector/emitter doping density of 5×10^{15} cm^{-3} (doping profile #2). This device has a responsivity of 10.42 A/W at 3 V, which is approximately two-thirds of its In$_{0.52}$Al$_{0.48}$As/In$_{0.53}$Ga$_{0.47}$As counterpart, at the gain of a lower dark current, as can be seen in Fig. 3. The lower dark current in the InP/In$_{0.53}$Ga$_{0.47}$As structure is due to: (i) a two-dimensional electron gas accumulation at the n^{++}–N^{++} isotype heterojunction contact layer interface; and (ii) a larger Early effect in the base of the In$_{0.52}$Al$_{0.48}$As/In$_{0.53}$Ga$_{0.47}$As device, caused by a larger built-in potential at the p-N anisotype heterojunction.

Another important consideration is the effect of the highly doped emitter side interface layers on device performance. Fig. 2
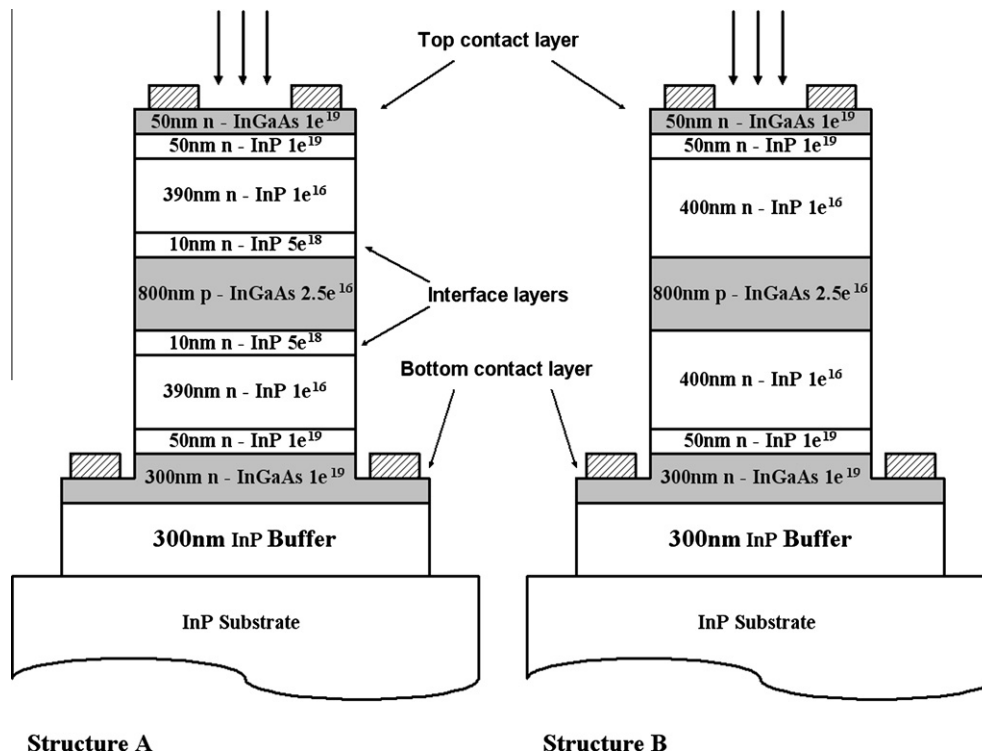

Fig. 1. The structures of the two InP/In$_{0.53}$Ga$_{0.47}$As heterostructure based symmetric gain optoelectronic mixers. Structure A with and B without the emitter-side highly doped interface layers.
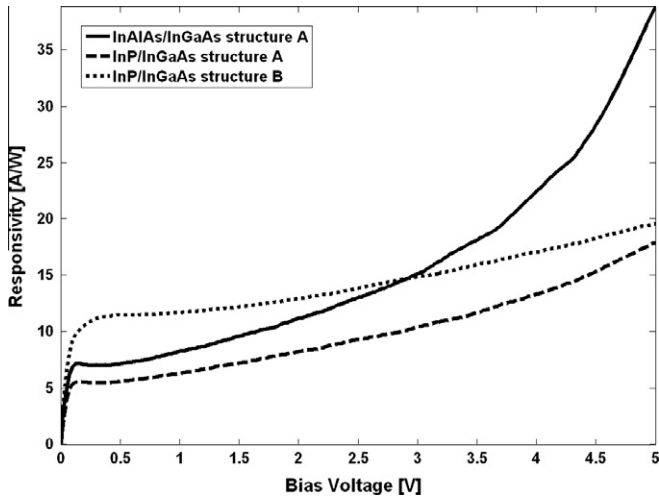
Fig. 2. Responsivity versus bias voltage for InP/In$_{0.53}$Ga$_{0.47}$As and In$_{0.52}$Al$_{0.48}$As/In$_{0.53}$Ga$_{0.47}$As based symmetric phototransistors with the same layer thickness and doping profile. Both structure A and B are included for InP/In$_{0.53}$Ga$_{0.47}$As based structures.
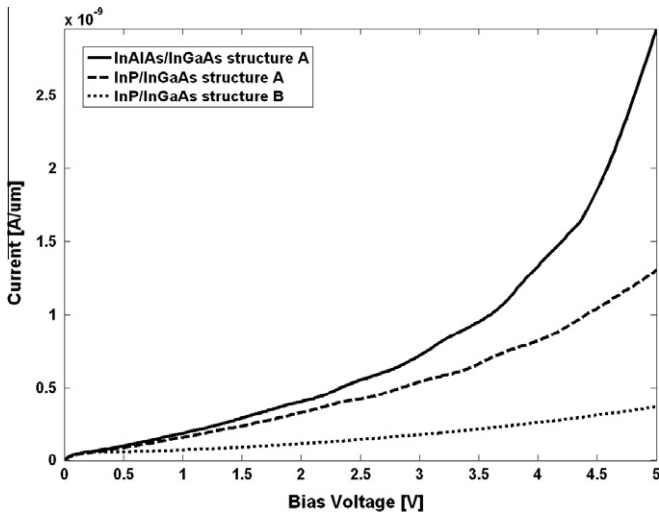

Fig. 3. Dark current versus bias voltage for InP/In$_{0.53}$Ga$_{0.47}$As and In$_{0.52}$Al$_{0.48}$As/In$_{0.53}$Ga$_{0.47}$As based symmetric phototransistors with the same layer thickness and doping profile. Both structures A and B are included for InP/In$_{0.53}$Ga$_{0.47}$As based structures.

compares the responsivity of structure A (with the interface layers) and structure B (without these layers) as a function of the bias voltage. Both structures have base thickness of 800 nm and doping densities of 2.5×10^{16} cm^{-3} in the base and 5×10^{15} cm^{-3} in the emitter/collector layers. Structure B is predicted to have a larger responsivity than structure A at low bias voltages. Figs. 2 and 3 also show that structure B is less susceptible to the Early effect, and has lower dark current. The weaker Early effect for structure B is due to the lack of the highly doped emitter–base interface layer. In structure A, the highly doped (10 nm, 10^{18} cm^{-3}) emitter interface layers cause most of the depletion region to extend into the base. In contrast, the depletion region is smaller in the base for structure B, which lacks these interface layers.

Base thickness and the doping densities of the base and emitter/collector layers are key SG-OEM design parameters. These parameters were systematically varied across a series of simulations to investigate their effects on device performance. Table 2 lists three doping profiles out of this data set, #1 and #3 being at the ex-

Table 2
Doping profiles of three sample structures.

	Doping profile 1	Doping profile 2	Doping profile 3
Base doping	1×10^{16} cm^{-3}	2.5×10^{16} cm^{-3}	5×10^{16} cm^{-3}
Emitter/collector doping	5×10^{16} cm^{-3}	5×10^{15} cm^{-3}	5×10^{15} cm^{-3}

tremes, and #2 being the optimum doping profile. Fig. 4 shows the DC responsivities of seven InP/In$_{0.53}$Ga$_{0.47}$As SG-OEMs based on structure A with doping profile #2, and base thicknesses ranging from 500 nm to 1100 nm. It should be noted that the device shown in Fig. 2 had the same doping profile. SG-OEM responsivity decreases with increasing base thickness, as the transistor gain decreases faster than the increase in the absorption with increasing base thickness in this range. To a first order, the responsivity, R, is proportional to:

$$R \propto \frac{(1 - e^{-\alpha d})}{d^2} \qquad (1)$$

where α is the absorption coefficient and d is the thickness of the base region, relating responsivity to the base width dependence of transistor gain. In contrast, increasing base thickness reduces base width modulation, i.e. the Early effect, and correspondingly increases the base punch-through breakdown voltage. Narrow base width devices (600 nm and below) are predicted to fail at bias voltages below 4 V due to punch-through breakdown. Fig. 5 shows the DC responsivity of three InP/In$_{0.53}$Ga$_{0.47}$As SG-OEMs based on structure B, with base thickness of 700 nm, 800 nm and 900 nm. Except for the interface layers, they have the same #2 doping profile. Similar to the structure A devices, the responsivity decreases with increasing base thickness. In general, the structure B devices have better responsivity, and lower susceptibility to the Early effect of their counterparts, and provide a better SG-OEM device.

Fig. 6 compares the responsivities of 800 nm base InP/In$_{0.53}$Ga$_{0.47}$As SG-OEMs with the three doping profiles given in Table 1. Device A.1 has the largest responsivity below 5 V, which is 13.42 A/W at 1 V and 38.81 A/W at 2 V, compared to 6.312/8.194 for A.2, and 4.564/8.194 for A.3. However, the abrupt jump in the responsivity at 3 V is due to base punch-through breakdown, which makes device A.1 unsuitable for practical applications. This low voltage base punch-through in A.1 is caused by the emitter/
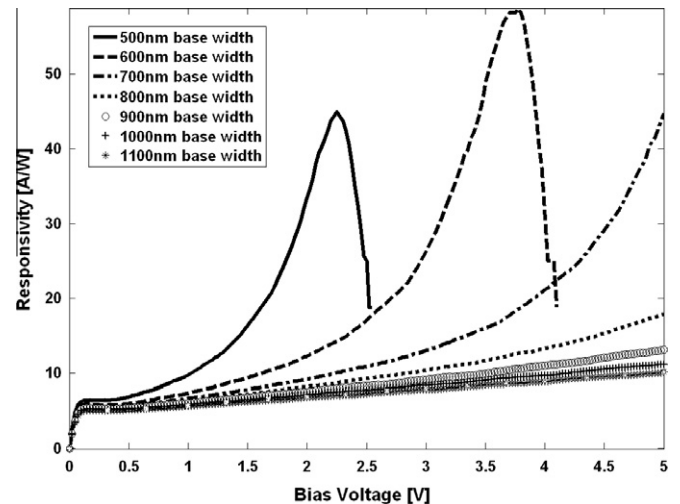

Fig. 4. Responsivity of structure A.2 as a function of base thickness. The base thicknesses range from 600 nm to 1000 nm.
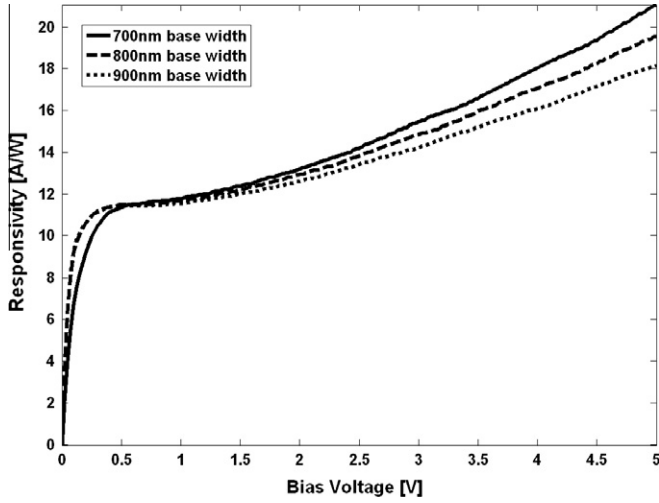
Fig. 5. Responsivity of structure B.2 as a function of base thickness. The base thicknesses range from 600 nm to 1000 nm.

Fig. 6. Responsivity of structure A as a function of the doping profiles given in Table 1. Base thickness is 800 nm.

collector doping density being larger than the base doping density, which causes the depletion region to extend mostly into the base.

Device B.2 with 800 nm base (Fig. 5) has a satisfactory responsivity (14.88 A/W at 3 V) in the low voltage range and does not suffer from punch-through breakdown below 5 V, the operational range of the devices. This responsivity value corresponds to 58,125 µA/W µm² when normalized by area. In comparison, Aliberti et al. reported a responsivity of 99 µA/W µm² at 3 V for an InGaAs MSM optoelectronic mixer with 1 µm thick absorption region [5]. Thus, the proposed SG-OEM devices are predicted to have approximately 580 times higher responsivity per unit area.

2.2. AC simulation and device modeling

Two major contributors to the SG-OEM's frequency response will be base transit time and the junction capacitances of the base-emitter/collector junctions. A set of small signal simulations were carried out to determine the total capacitance seen by the LO signal driving the SG-OEM for both structures A and B, with doping profile #2 and base thicknesses of 600 nm and 800 nm. Table 3 lists the device dimensions used for these simulations. The small signal superimposed on the DC bias has a frequency of 1 MHz. Simulations were carried out for dark conditions, and under an optical illumination of 1 mW/cm².

Fig. 7 shows total capacitance versus bias voltage of the two device structures. The total capacitance seen at the terminals for devices A and B are about 7 fF and 2.5 fF at zero bias and dark conditions, respectively, which decreases in all four devices as the bias voltage increases. This is due to the decrease of reverse biased pn junction capacitance with increasing bias voltage:

$$C = \sqrt{\frac{qN_{A,B}N_{D,EC}\varepsilon_B\varepsilon_{EC}}{2(N_{A,B}\varepsilon_B + N_{D,EC}\varepsilon_{EC})(V_{bi} + V_R)}} \qquad (2)$$

where $N_{A,B}$ and $N_{D,EC}$ are the doping density of base and emitter/collector, respectively, ε_B is the relative permittivity of the InGaAs base and ε_{EC} that of the InP emitter/collector, V_{bi} is the built-in barrier, V_R is the bias voltage and q is unit charge. The peak at 4 V for the structure A device with 600 nm base width is due to punch-through breakdown, consistent with DC responsivity simulations. The total capacitance decreases slightly with increasing base thickness. This dependence on the base thickness is weakened by the emitter-side highly doped interface layer for structure A, which reduces the extension of the depletion region into the emitter/collector layers,
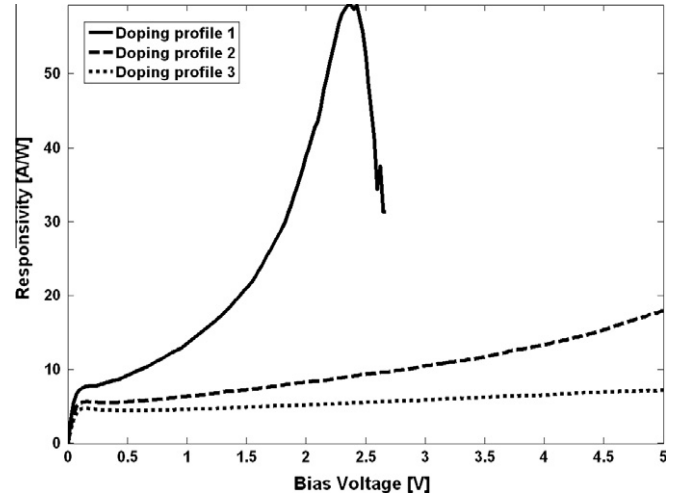
Table 3
Device dimensions used in the simulations.

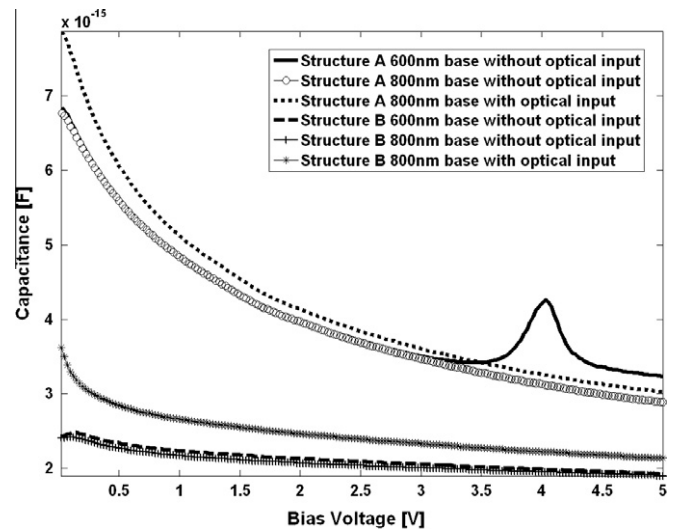| Parameter	Size (µm)
Inner mesa	16
Outer mesa (bottom contact)	30
Top contact width	12
Top contact metal width	14
Bottom contact width	2
Bottom contact metal width	5

Fig. 7. Total capacitance of structure A.2 and structure B.2 as a function of base thickness.

and thus leaves the capacitance almost unchanged with the variation in the base width. Also displayed in Fig. 7 are the simulated capacitance curves of 800 nm base width devices, under an optical illumination of 1 mW/cm². Capacitance values shift upwards approximately 0.3–0.5 fF under illumination. Structure B devices will provide a better frequency performance, due to their lower overall capacitance.

Fig. 8 shows the equivalent circuit model for the two terminal symmetric gain optoelectronic mixer. The current source represents the photocurrent ($\mathcal{R}P_{opt}$). The forward and reversed biased
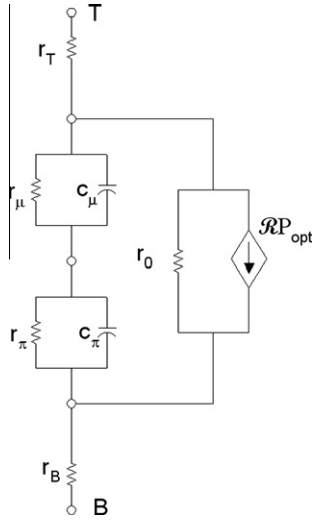
Fig. 8. Equivalent circuit model of an SG-OEM device.

junction capacitances are represented by C_μ and C_π, respectively. The resistor r_0 represents the Early effect. The series resistances of the top emitter/collector layers are represented by r_T, and that of the bottom by r_B.

For structure B, doping profile 2, the total capacitance seen between the two terminals at 0 V bias is calculated to be 2×10^{-15} F/μm using Eq. (2), while the simulation result is 2.4×10^{-15} F/μm. The discrepancy is mainly due to the highly conductive contact layers, which cause a narrowing of the depletion region in the emitter/collector layers. The top layer series resistance, r_T, is dominated by the heterojunction formed by the n++ InGaAs/N++ InP contact layers. The current mechanism through this barrier is tunneling (field emission), as the two layers are highly doped (10^{19} cm^{-3} and 10^{18} cm^{-3}, respectively). This resistance is predicted to be approximately 260 Ω μm. The bottom layer series resistance, r_B, is dominated by the narrowing of the contact layer after the mesa etch step. At high current levels, when current crowding in the narrowing contact layer becomes an issue, this resistance is predicted to be approximately 5.7 kΩ μm, assuming the contact layer is etched mid-way. This resistance will be dependent on accurate control of the inner mesa etch step in the device fabrication process.

3. Conclusion

InP/In$_{0.53}$Ga$_{0.47}$As based SG-OEMs are a promising replacement for In$_{0.52}$Al$_{0.48}$As/In$_{0.53}$Ga$_{0.47}$As SG-OEMs, due to reduced defect densities in the materials, and being less susceptible to the Early effect and punch-through break down. Two-dimensional device simulations were used to optimize device structure over base width, base and emitter doping, and emitter/base interface layers. It was determined that highly doped interface layers caused an increase in dark current and device capacitance and also lowered the base punch-through breakdown voltage. An optimized device structure was ordered for material growth and device fabrication, to be presented in a future publication.

References

[1] Stann BL, Aliberti K, Carothers D, Dammann J, Dang G, Giza M, et al. A 32 × 32 pixel focal plane array ladar system using chirped amplitude modulation. Laser Radar Technol Appl IX Proc SPIE 2004;5412:264–72.
[2] Ruff W, Bruno J, Kennerly S, Ritter K, Shen P, Stann B, et al. Self-mixing detector candidates for an FM/cw ladar architecture. Laser Radar Technol Appl V, Proc SPIE 2000;4035:152–62.
[3] Choi CS, Seo JH, Choi WY, Kamitsuna H, Ida M, Kurishima K. 60-GHz bidirectional radio-on-fiber links based on InP–InGaAs HPT optoelectronic mixers. IEEE Photon Technol Lett 2005;17(12):2721–3.
[4] Shen H, Aliberti K. Theoretical analysis of an anisotropic metal–semiconductor–metal opto-electronic mixer. J Appl Phys 2002;91(6):3880–90.
[5] Shen H, Aliberti K, Stann B, Newman P, Mehandru R, Ren F. Mixing characteristics of InGaAs metal–semiconductor–metal photodetectors with Schottky enhancement layers. Appl Phys Lett 2003;82(22):3814–6.
[6] Shen H, Aliberti K, Stann B, Newman PG, Mehandru R, Ren F. Analysis of InGaAs metal–semiconductor–metal OE mixers. Phys Simulat Optoelectron Dev XII Proc SPIE 2004;5349:197–205.
[7] Emanetoglu NW, Drew S, Bambha N, Bickford JR. Symmetric gain optoelectronic mixers for LADAR. In: Proc of the 2008 US army science conference. NP-11; December 2008.